Materials Science Forum
ISSN: 1662-9752, Vol. 1062, pp 69-73
doi:10.4028/p-54nqrc

Submitted: 2021-10-15
Revised: 2022-03-16
Accepted: 2022-03-17
Online: 2022-05-31

Impact of N Doping on 3C-SiC Defects

Cristiano Calabretta[1,a*], Viviana Scuderi[1,b], Annalisa Cannizzaro[1,c], Ruggero Anzalone[2,d], Marco Mauceri[3,e], Danilo Crippa[4,f], Simona Boninelli[1,g], and Francesco La Via[1,h]

[1]CNR-IMM, VIII Strada, 5, 95121 Catania, Italy

[2]STMicroelectronics, Stradale Primosole 50, 95121 Catania, Italy

[3]LPE, Strada XVI, Catania, Italy

[4]LPE, via Falzarego 8 Baranzate (MI), Italy

[a*]cristiano.calabretta@imm.cnr.it, [b]viviana.scuderi@imm.cnr.it, [c]annalisa.cannizzaro@imm.cnr.it, [d]ruggero.anzalone@st.com, [e]marco.mauceri@lpe-epi.com, [f]danilo.crippa@lpe-epi.com, [g]simona.boninelli@imm.cnr.it, [h]francesco.lavia@imm.cnr.it

Keywords: 3C-SiC; Stacking Faults; Dislocations; Molten KOH; Defect reduction; nitrogen doping; SEM.

Abstract. This work studies the variation of the defects density of in situ doped 3C-SiC layers during heteroepitaxial Chemical Vapour Deposition (CVD). A review on the evolution of defects density as a function of 3C-SiC grown thickness, for different N doping concentrations is offered. The doping range spanned in the experiment suits the realization of power devices.

The outcome of this work provides an explanatory picture of the significant drop in stacking faults density by roughly an order of magnitude through the N doping at concentrations of the order of ~2.9×10^{19} cm^{-3} during the growth. Conversely, N doping shows to favor the development of dislocation-like defects within the crystalline matrix. However, in few μm, the crystal is able to display an effective dislocation closure mechanism, which rapidly recovers crystal quality.

Introduction

3C-SiC is a particularly attractive SiC polytype since it has higher mobility and a lower density of states at the 3C-SiC/SiO_2 interface than 4H and 6H-SiC. These characteristics, along with 2.5 eV bandgap, make 3C-SiC suitable for power electronic applications, due to several benefits in MOS devices such as a notable R_{on} reduction for medium voltage applications working under 1200 V [1].

Current technology is largely based on Si heteroepitaxial growth which involves 20% mismatch in the lattice parameter and 8% different thermal expansion coefficient. As a consequence, several types of defects, such as dislocations and stacking faults (SFs) nucleate close to the 3C-SiC/Si interface, both during the high temperature deposition and the cooling down, driven by the misfit strain relaxation [2-3]. Such defects hinder 3C-SiC device realization and provide significant leakage sources that are incompatible with large-scale integration (VLSI) technology.

So far, compliant substrates have been involved in preventing stacking faults, usually found at the SiC/Si interface, from reaching the surface [4]. Up to now, studies have been focused on the trend of dopant incorporation as a function of the growth parameters and on the evidences of conductivity [5-6], however investigation on the effect induced by CVD doping on 3C-SiC crystal defects have been rare [7-8].

This work provides an innovative detailed examination of nitrogen (N) doping impact over crystal, following defect evolution along grown layers based on molten KOH etching applied on uniformly lapped samples at an angle of 1.9° from sample backside.

Materials and Methods

3C-SiC growth was performed in a horizontal hot-wall Chemical Vapour Deposition (CVD) reactor using (100) oriented 4° off-axis with <110> off-cut Si substrates. Precursor gases were Tri-chloro-silane (TCS) and Ethylene (C_2H_4) with (H_2) as carrier gas. A two-step growth process was applied with the carbonization plateau at 1160 °C followed by CVD growth step at 1400 °C. One 4-inches wafer was grown intrinsic while other growths were carried out with constant 314, 800 and 1600 sccm N_2 fluxes. To increase crystal quality, the process was first performed at a low growth rate of 3 µm/h for 30', followed by another 30' growth at 6 µm/h and then fast growth rate of 30 µm/h was carried out until a ~ 70 µm layer was reached. Afterwards, Si substrate was melted at 1600 °C in the reactor to reach a free-standing wafer. Secondary Ion Mass Spectroscopy (SIMS) investigation led to N concentrations of 1.2×10^{19}, 2.9×10^{19}, 5.8×10^{19} cm^{-3}. Molten KOH etching at 500 °C for 3' was performed on uniformly lapped sample at an angle of 1.9° from sample backside in order to provide a comprehensive examination of crystal defects from the initial growth layers up to thicknesses of 40 µm through SEM microscopy in-plane analysis.

Discussion

Through the molten KOH etching process, SFs are visually highlighted and are revealed as lines that stand out from the non-defective crystal, while dislocations present inside the crystal are enhanced in the form of pits.

Particularly impressive SFs density variation is visually attested in Fig. 1, which exhibits two SEM images of intrinsic and 5.8×10^{19} cm^{-3} doped sample, in Fig. 1a) and 1b), respectively, acquired at 30 µm growth depth post molten KOH etching. The appearance of SFs in a single direction is driven by preferential etching following binding energy difference within Si-terminated SF (SF_{Si}) and C-terminated ones (SF_C).

In Figure 1a there is a noticeable presence of SFs and two examples are enclosed by red dashed lines. On the other hand, in Fig. 1b a reduced number of SFs are present, but with the appearance of etch pits. Two examples of etch pits which are usually linked to dislocations are indicated by yellow dashed circles.

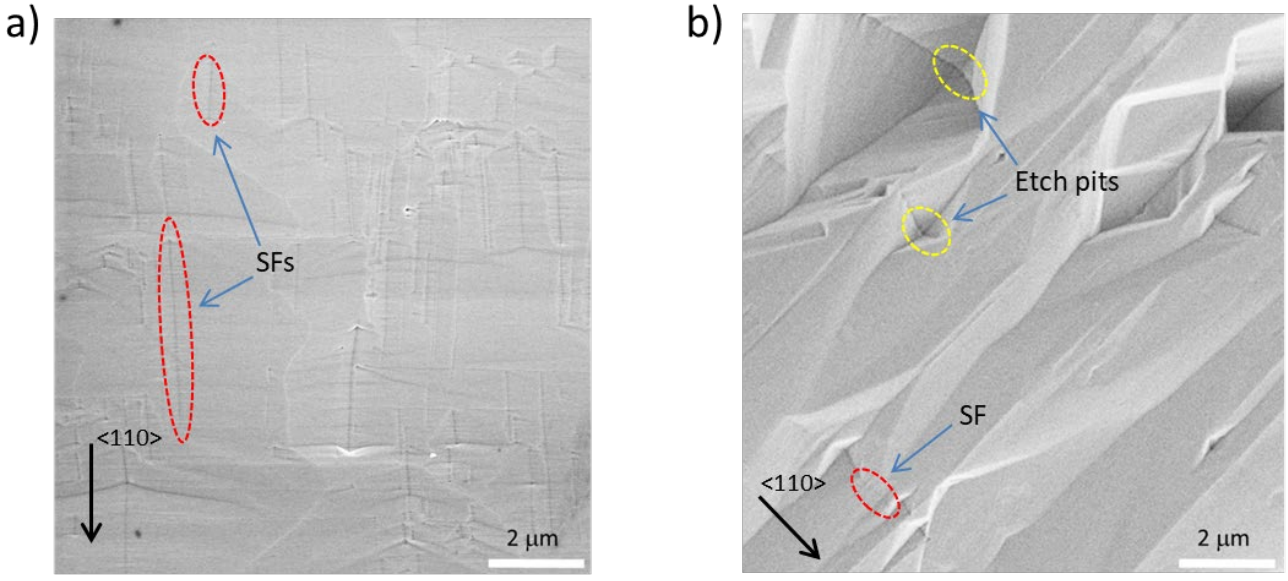

Figure 1. SEM micrograph acquired at the growth thickness of 30 µm of a) an intrinsic sample and of b) a sample doped at 5.8×10^{19} cm^{-3} subjected to molten KOH etching.

Within Figures 2a and b the results coming from decaying exponential fits arising from the measurements of the SFs and etch pits densities are represented. Figures 2a and b show, in particular, the 95% confidence curves of the exponential fits extracted from the experimental densities data with respect to the grown 3C-SiC layer thickness, from interface to 40 µm thickness. Fig 2a shows the intrinsic sample (grey band) following a constant SFs concentration trend, whose density range goes from $(1.3\pm0.5)\times10^{4}$ cm^{-1} at 0 µm to $(9.7\pm0.9)\times10^{3}$ cm^{-1} at 50 µm. This trend is followed by the SFs size evolution, which goes from an average value of ~ 0.25 µm at the interface to ~ 2.5 µm in length at 50 µm growth (not shown). Conversely, the introduction of N into the chamber drives a remarkable SFs density decrease, from the first layers. Based on the observations of the lowest and highest doped samples, at the interface the SFs concentration are fairly comparable attesting on $(3.6\pm0.7)\times10^{3}$ SFs×cm^{-1} for the lower doped sample (red band in the graph) and of $(2.8\pm0.2)\times10^{3}$ SFs×cm^{-1} for higher doping (violet band in the graph). Indeed, in the first µm the density contribution from both crystals is highly influenced by the low growth rate involving lower SFs generation. The subsequent growth rate rising to 30 µm/h responds to a slight increase in the SFs density during the low doped growth, while in the case of higher N_2 flow, an exponential-decay trend involves SFs density to stabilize at $(7.9\pm0.4)\times10^{2}$ SFs×cm^{-1} already at 40 µm. The comparison between these two apparently contrasting trends responds to the different dopant concentrations incorporated in the crystal.

From calculations made using Vienna Differential Functional Theory it is evident that N favors the increase of the formation energy of SFs. As a result, assuming that the dopant effect appears when it is inside or close to the SF [9] the significant decrease in SFs density is explained by increased N incorporation in the crystal matrix. Moreover, it is worth noting that when subjected to intermediate doping 2.9×10^{19} cm^{-3}, the crystal matrix undergoes lower SFs generation in the first 10 µm due to a longer exposure to low growth rates during CVD growth.

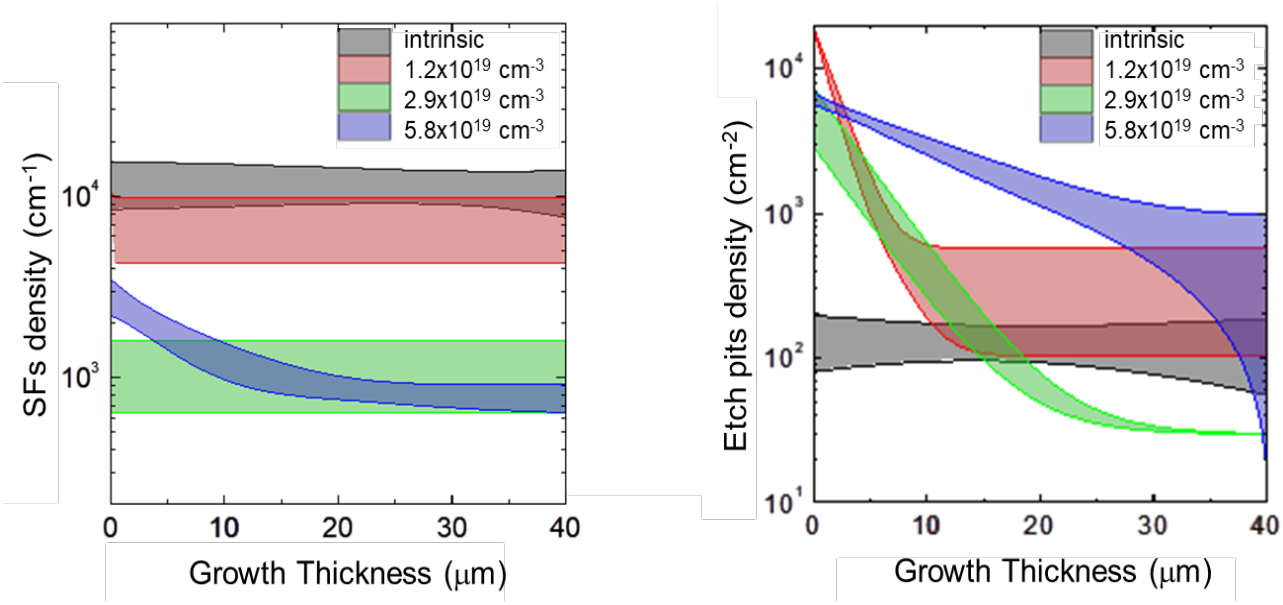

Figure 2. The 95% confidence curves of the decaying exponential fits plotted by the density data of SFs a) and etch pits b) as a function of the growth 3C-SiC thickness.

Nevertheless, it is evident that from 20 µm growth higher SF closure mechanism prevails in the highest doping regime. It is worth noting, however, that if the misfit stress between 3C-SiC and Si substrate is effectively contained by carbonization steps in intrinsic growth, rapid multiplication of dislocations and progressive increase in dislocations density with growing strain is testified in the doped samples from Figure 2b. In fact, the relaxation of the compressive stress accumulated consequently to the doping incorporation occurs through the generation and gliding of dislocations

whose density increases with the N_2 flow in CVD chamber. Etch pits density in the intrinsic sample is just over 100 etch pits×cm^{-2}, while in the most doped samples (6.2±0.5)×10^3 etch pits×cm^{-2} at 0 μm are observed up to (5.5±0.2)×10^2 at 40 μm growth thickness. It is interesting to note that the density falls below the value recorded in the intrinsic growth in the case of the sample with medium doping from 15 μm depth. The identification and atomic structure of the dislocations revealed by the etch pits were exhaustively investigated in [10], as well as μ-PL cross-section maps of the band-to-band peak intensity located at 540 nm performed for the intrinsic and heavily doped samples along the entire grown thickness. The map of the doped sample showed how the band-to-band peak grows faster and more homogeneously in the most doped sample than in the intrinsic one, confirming the improved quality of the grown crystal through doping. As a result of the foregoing, it is possible to assert that 3C-SiC crystal quality strongly benefits from suitable N doping, since the first grown layers and further strategies to shrink the dislocations density in the early stages of growth can include growth rates tuning and N supplied concentration as well as generation of physical opposite dislocations.

Acknowledgements

This research was funded by SiC Nano for PicoGeo project, European Union's Horizon 2020 research and innovation programme under grant agreement No. 863220.

Summary

This paper provides a comprehensive description of the N doping effect on 3C-SiC epitaxial layers. It demonstrates that the crystal is highly sensitive to N doping concentration in the range of 2×10^{19} cm^{-3} and significantly lowers the density of SFs by an order of magnitude.

The addition of N doping within the growth chamber increases the concentration of dislocation-like defects within the initial growth layers; nevertheless, the density of these defects is rapidly decreased during growth in the first microns. This trend is beneficial for breaking down dislocation concentrations, below the densities measured inside the intrinsic crystal, leading in light of what stated for SFs to highly pure 3C-SiC crystal.

References

[1] F. La Via et al. New approaches and understandings in the growth of cubic silicon carbide, Materials, 14(18), 2021, 5348.

[2] M. Zimbone et al., Generation and Termination of Stacking Faults by Inverted Domain Boundaries in 3C-SiC, Crystal Growth and Design, 20(5), 2020, 3104-3111

[3] M. Zimbone et al. Extended defects in 3C-SiC: Stacking faults, threading partial dislocations, and inverted domain boundaries, Acta Materialia, 213, 2021, 116915.

[4] M. Zimbone et al. 3C-SiC growth on inverted silicon pyramids patterned substrate, Materials, 2019, 3407.

[5] M. Zielinski et al. Nitrogen doping of 3C-SiC thin films grown by CVD in a resistively heated horizontal hot-wall reactor, Journal of Crystal Growth, 310,2008, 3174-3182.

[6] H.K.E. Latha et al., Microstructure and electrical properties of nitrogen doped 3C–SiC thin films deposited using methyltrichlorosilane, Materials Science in Semiconductor Processing, 29,2015, 117-123.

[7] V. Scuderi et al. Characterization of 4H-and 6H-like stacking faults in cross section of 3C-Sic epitaxial layer by room-temperature μ-photoluminescence and μ-raman analysis, Materials

[8] C. Calabretta, et al. Effect of Nitrogen and Aluminum Doping on 3C-SiC Heteroepitaxial Layers Grown on 4° Off-Axis Si (100), Materials, 14(16), 2021, 4400.

[9] Y. Umeno, K. Yagi, and H. Nagasawa, Phys. Status Solidi B, 1–6, (2012).

[10] C. Calabretta et al. Impact of nitrogen doping on the selective closure of Stacking Faults in 3C-SiC, Journal of Materials Science (submitted).